Progress with the analysis of dimethyl ether sprays with a moments spray model

N.G. Emekwuru
Midlands Simulation Group, School of Technology, University of Wolverhampton, United Kingdom.
n.emekwuru@wlv.ac.uk

Abstract

The representation of spray characteristics in internal combustion engines using spray models has taken on greater significance with the increased need to reduce engine emission levels. Apart from work on improving existing diesel and gasoline engines, research on evaluating other fuel types, including dimethyl ether, for internal combustion engines has intensified. Thus, existing fuel spray models, developed for diesel engine spray assessments for example, have to be applicable to the new fuel types being investigated. A diesel spray model has been developed that represents diesel sprays by means of three moments of the droplet-size distribution function calculated from transport equations and one moment obtained from a Gamma size distribution. The applicability of the moments diesel spray model is analysed for dimethyl ether sprays. The results are characterized by dimethyl ether spray tip penetration at different injection nozzle sizes and ambient pressure values. These are compared with experimental data. The results indicate that the moments spray model can be applied as a predictive tool for dimethyl ether spray tip penetration. However, there are discrepancies in the observed and predicted penetration values at early and late injection times. Thus, it might still be useful to develop initial injection correlations specific to dimethyl ether spray simulations.

Introduction

Emissions from internal combustion engines are a global concern. For instance, diesel fuel engine vehicles are considered to be a significant source of NO_x and particulate matter emissions. To combat these issues work on improving the existing diesel fuel engines has increased, but researchers are also increasingly studying alternative fuel types. Several alternative fuels like ethanol, methanol, compressed natural gas, and liquefied petroleum gas, have been investigated but manufacturing costs, environmental, health, and safety concerns have limited their usage. Some of the alternative fuels are also considered to be more suitable for spark ignition rather than for compression ignition engines [1-2]. However, dimethyl ether (DME) has been recognised as a suitable alternative fuel to diesel for better combustion and less pollutant formation [3]. Its cetane number (55-60) is close to that of diesel fuel (45-55), making it suitable for use in existing diesel engines without extensive modifications [4]. DME powered vehicles have been built with maximum speed and acceleration performance equivalent to those obtained from diesel engine powered vehicles but with lower noise levels [1-2].

The numerical investigations of the characteristics of DME sprays have generally followed the same pattern as in the practical investigations; existing diesel spray models have been modified to assess the characteristics of DME sprays. Many diesel sprays models are based on the discrete droplet model (DDM) introduced by Dukowicz [5]. In this model the equations of the turbulent carrier gas motions are computed in an Eulerian scheme, while the equations of the liquid droplet motions are computed using a Lagrangian scheme along true path lines. These two schemes, and therefore the liquid and gas phases, are linked using source terms in the transport equations. Modified diesel spray models using this DDM approach have been applied to DME sprays [6-8], and the results indicate that these models can be applied to DME spray characterisation.

This paper presents the progress made with applying an alternative diesel spray model [9-10] to characterising DME sprays. This is based on a moments spray model in which the first four moments of the droplet size distribution are used to describe the distribution of the droplet sizes. The last three moments in this model are predicted from transport equations, while the first moment is calculated from a general Gamma distribution function. This numerical method of evaluating sprays is more computationally efficient than the DDM method as the computationally intensive process of tracking the chaotic motions of the individual droplets is avoided. The model has been extensively treated elsewhere [11-12]. The results are presented in terms of spray tip penetration. The prediction of spray tip penetration is of considerable practical importance in internal combustion engines because it is a strong function of several operating parameters in engines including injection pressure, ambient density, and nozzle geometry [13]. The next section of the paper introduces the summary of the numerical basis of the moments spray model. The third section discusses the results from the model for DME spray tip penetration, and finally the summary and conclusions are highlighted.

Numerical Methods

The main difference between the moments based spray model and those using the DDM approach is that the former presents the characteristics of sprays without solving the equations of motions of groups of droplets of equal size like the later. The approach used for the moments spray model is presented next.

Moments of the droplet number probability distribution

The moments of the droplet number probability distribution is defined as

$$Q_i = \int_0^\infty n(r) r^i dr \tag{1}$$

The first four moments, Q_0 to Q_3, are used in this model:

- Q_0 is the total number of droplets (the droplet number moment),
- Q_1 is the total sum of radii of the droplets,
- $4\pi Q_2$ is the total surface area of the droplets and,
- $\frac{4\pi Q_3}{3}$ is the total volume of the droplets, all per unit total volume.

The treatment of the general Gamma distribution to represent droplet size distributions is treated in reference [14].

The moment transport equations

The last three moments, Q_1 to Q_3, are calculated by solving the transport equations for the moments. The set of the moment transport equations (for i = 1, 2, 3), can be written compactly as:

$$\frac{\partial}{\partial t}(Q_i) + \frac{\partial}{\partial x_j}(Q_i U_{lij}) = -S_{Q_i} \tag{2}$$

Also, the respective liquid-phase momentum equations can be written compactly as:

$$\frac{\partial}{\partial t}(Q_i U_{lij}) + \frac{\partial}{\partial x_k}(Q_i U_{lij} U_{lik}) + U_{l3j} B_{Q_i} + U_{lij}(S_{Q_i} - B_{Q_i}) = \frac{\partial}{\partial x_k}\left(Q_i \sigma_v \nu_l \frac{\partial U_{lij}}{\partial x_k}\right) - S_{U_{lij}} \tag{3}$$

The subscript k denotes the moment number, and σ_v is the coefficient of Melville and Bray [21].

The source terms

$S_{U_{lij}}$ represents the effects of the drag on the droplet momentum,

S_{Q_i} represents the effects of the droplet breakup, droplet collisions, and evaporation on the moments, and,

B_{Q_i} represents the break-up part of S_{Q_i}.

The forms of these source terms are presented in [12].

Droplet size distribution

The first moment, Q_0, is calculated from a Gamma distribution function. This function can be described in terms of a shape parameter k, and a scale parameter x, by the integral:

$$\Gamma(k) = \int_0^\infty e^{-x} x^{k-1} dx \tag{4}$$

The moments of this distribution are given by:

$$Q_i = Q_0 \int_0^{\infty} \frac{\alpha^k}{\Gamma(k) r_{32}^k} r^{k+i-1} e^{-\alpha\left(\frac{r}{r_{32}}\right)} dr \tag{5}$$

The partial integration of equation (5) leads to

$$Q_0 = \frac{(k+2)}{k r_{32}} Q_1 \tag{6}$$

The advantages of this method include the calculation of less transport equations in the model and the use of the Gamma distribution function to describe the inlet conditions, the form of the drag model, and the break-up and collision models [12].

Solution and discretization

The transport equations are written for the last three moments, while the first moment is calculated from the general Gamma distribution function (see equation (6)). The velocities used in the transport equations are calculated from moment-average velocities, and solving the transport equations for the relevant moment-average momentum. The spray model is closed by equations for the energy of the liquid phase and gas-phase equations. All the equations are solved using an Eulerian scheme, and discretized using the finite volume approach. The spray cases are considered axisymmetric. An Euler implicit method is used for the temporal differencing while a hybrid central/upwind scheme is used for the spatial differencing. The carrier gas is considered turbulent and the $k-\varepsilon$ (turbulent kinetic energy - dissipation rate) model of Launder and Spalding [15] has been used. The details of the moments model have been extensively discussed in reference [12].

Results and Discussion

The penetration data used for validating the progress of the model is from the work of Kim *et al.* [13]. This work was of particular interest because the authors applied 5 [16-20] different zero-dimensional diesel spray penetration models to their DME fuel spray tip penetration experiment data, and concluded that the models can be used to analyse DME spray tip penetration. Thus, this forms a useful basis for assessing the DME fuel spray penetration data from the moments model.

Experimental data

Kim *et al.* [13] injected DME sprays into a high-pressure chamber filled up with Nitrogen, at ambient pressure values of 0.6, 1.0, and 1.5 MPa. The spray tip penetration was measured using a Particle Motion Analysis System (PMAS). The edge of the spray was defined as a line of 80% transmittance. Some of the experimental conditions are presented in Table 1.

Table 1: Experimental conditions for the data of Kim *et al.* [13].

	Case 1	Case 2	Case 3	Case 4	Case 5	Case 6
Ambient Pressure (MPa)	0.6		1.0		1.5	
Injection Pressure (MPa)	35.0		35.0		35.0	
Nozzle Diameter (mm)	0.2	0.4	0.2	0.4	0.2	0.4

Numerical parameters

The two-dimensional computational grid used for the model is presented in Figure 1. The number of grid cells chosen was based on an earlier grid independence test [10] comprising of three different grids of 1944, 4779, and 7957 cells, respectively, and considering spray tip penetration simulation tests. As in [10], the grid used for this work comprises of 7957 cells but in a computational chamber 0.2 x 0.1m in size. Parametric tests for the variations of the computed spray tip penetration data with ambient pressure were performed and found to be similar to those in [9]; the model predicts that spray penetration decreases with increases in ambient pressure. These results are presented in Figure 2. Parametric tests for the variations of the computed spray tip penetration data with the orifice diameter were also performed and shown to indicate that the spray tip penetration increases with increase in orifice diameter (figure 3); this is as expected and further discussion regarding this is presented in the next section. The exact data from [13] were used wherever possible in the model. Table 2 presents the parameters used for the numerical calculations.

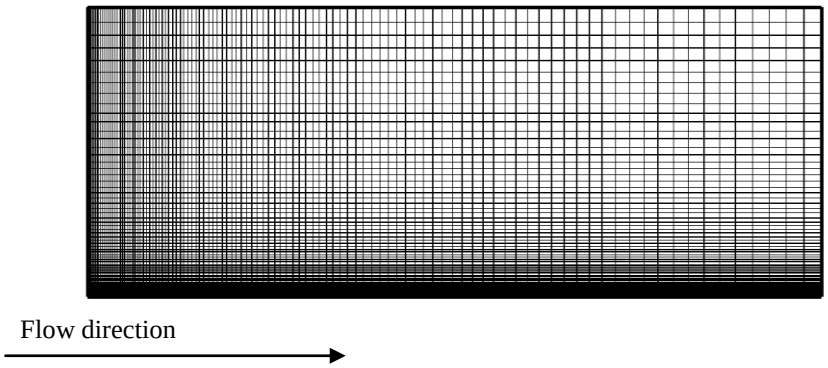

Figure 1: Grid used for the computational cases. The domain contains 7957 cells and is 200 mm long and 100 mm wide.

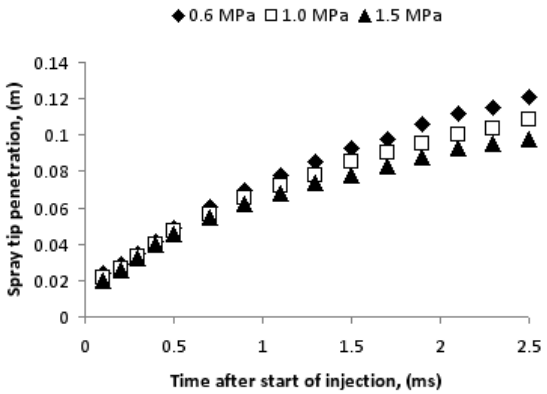

Figure 2: Variation in spray tip penetration with ambient pressure for an orifice diameter of 0.4mm, and injection pressure of 35 MPa.

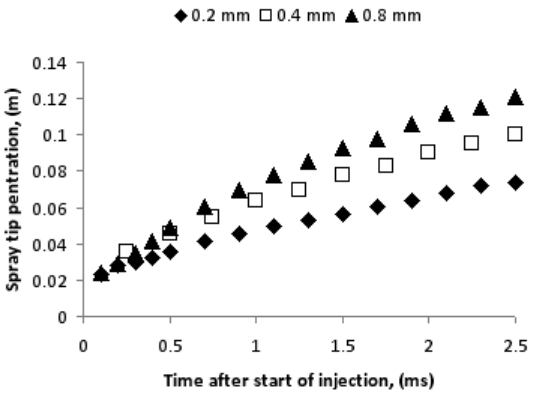

Figure 3: Variation in spray tip penetration with orifice diameter for an ambient pressure value of 0.6 MPa, and injection pressure of 35 MPa.

Table 2: Numerical, physical, and injection conditions used for the moments spray model to simulate the experiments of Kim *et al.* [13].

	Model Case 1	Model Case 2	Model Case 3	Model Case 4	Model Case 5	Model Case 6
Ambient Pressure (MPa)	0.6		1.0		1.5	
Injection Pressure (MPa)	35.0		35.0		35.0	
Nozzle Diameter (mm)	0.2	0.4	0.2	0.4	0.2	0.4
Chamber radius, (m)	0.100					
Chamber axial length, (m)	0.200					
Number of cells in axial direction	109					
Number of cells in radial direction	73					
Computational time step, (μs)	1					
Total computation time, (*ms*)	5					

Discussion

Data from the experiments of Kim *et al.* [13] indicate that spray tip penetration falls with increasing ambient pressure values for both injector orifice diameter (0.2 mm and 0.4 mm) cases. For instance for a time of 2.1 ms after the start of fuel injection, for the 0.2 mm orifice diameter, the spray tip penetration is measured at about 83 mm for the ambient pressure case of 0.6 MPa, 78 mm for the ambient pressure case of 1.0 MPa, and 66 mm for the ambient pressure case of 1.5 MPa (see figures 4a, 5a, and 6a). The results from the numerical simulations follow these trends (figures 4a, 5a, and 6a) and the parametric tests in the previous section also confirmed this (figure 2). With increases in ambient pressure, the gas density increases which results in the slowing down of the liquid droplets with the resultant decrease in spray penetration [9]. Thus the model behaves as expected.

Both the experimental and numerical data indicate that the wider orifice diameter cases show longer spray tip penetration for all the ambient pressure values tested. This observation is similar to the parametric tests reported in the previous section and presented in figure 3. For instance, at an ambient pressure of 1.5 MPa, the maximum reported experimental [13] spray tip penetration for the 0.2 mm orifice diameter case is about 76 mm (figure 6a), while it is about 85 mm for the 0.4 mm orifice diameter case (figure 6b). For the later case this was reported at 2.3 ms after the start of injection, whereas for the former at 2.9 ms. Therefore, the fuel has to be

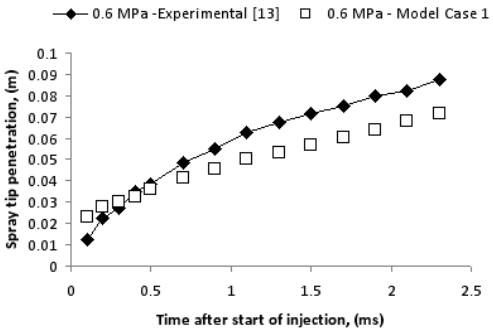

Figure 4a: Comparison of computed spray tip penetration with experimental data. Orifice diameter = 0.2 mm.

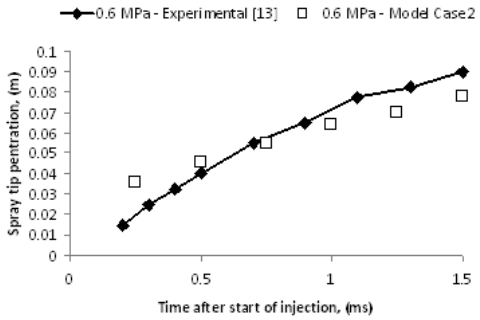

Figure 4b: Comparison of computed spray tip penetration with experimental data. Orifice diameter = 0.4 mm.

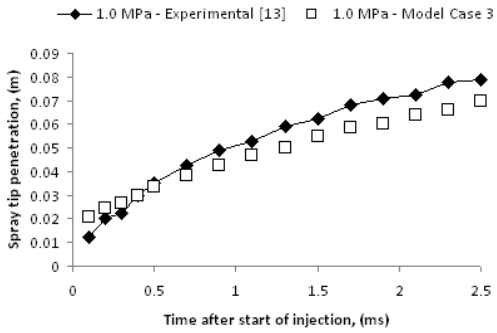

Figure 5a: Comparison of computed spray tip penetration with experimental data. Orifice diameter = 0.2 mm.

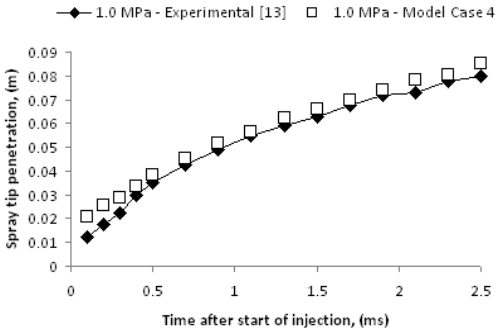

Figure 5b: Comparison of computed spray tip penetration with experimental data. Orifice diameter = 0.4 mm.

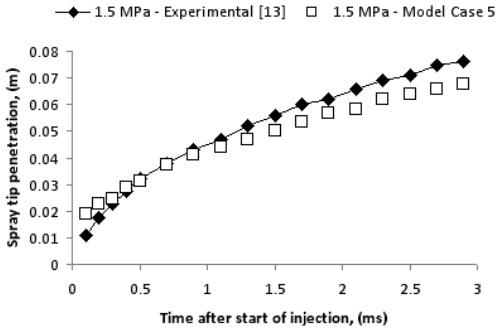

Figure 6a: Comparison of computed spray tip penetration with experimental data. Orifice diameter = 0.2 mm.

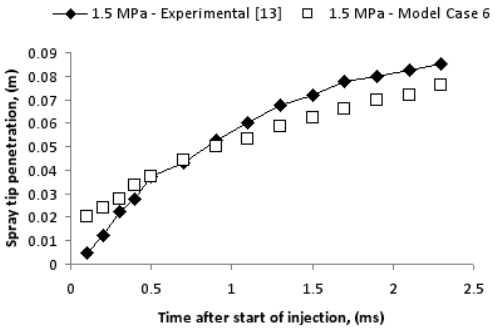

Figure 6b: Comparison of computed spray tip penetration with experimental data. Orifice diameter = 0.4 mm.

injected over a longer period for the narrower orifice diameter case to match the spray tip penetration for the wider orifice diameter cases. Increasing the orifice diameter has the effect of increasing the amount of fuel mass injected; this increases the liquid momentum and the spray tip penetration is increased. Thus, the model also behaves as expected in this aspect.

Analysis of the computational results indicate that the spray tip penetration results are generally over predicted compared to the experimental data at the start of the spray injection, and under predicted at late injection times (figures 4a to 6b). This trend is the same for all the ambient pressure cases and the two orifice diameter cases. The predictions improve with increases in ambient pressure (figures 4a to 6b). A number of factors may account for the discrepancy between the predicted and experimental spray tip penetration at the early injection times, the form of the drag model, the form of the droplet break up model, and the correlations at the initial injection stage, for instance. The models for these from the diesel spray model have not been modified at this stage, and experimental data for spray cone angles, initial spray velocity, or other initial injection parameters for DME sprays might be needed to implement a more satisfactory early injection spray tip penetration characterisation.

Another possible implication of the numerical results from figures 4 to 6 is that the model is predicting a larger number of larger sized droplets (hence faster and penetrating further) closer to the orifice, and a smaller number of smaller sized droplets (hence slower and penetrating less) compared to the experimental data. To validate this assumption would entail comparison of numerical data with experimental drop size data, but these were not available from the experimental data used. Therefore, apart from the initial injection correlations for the DME sprays, it might be worthwhile to investigate further the appropriateness of the use of droplet break up and coalescence models developed for diesel sprays models for use in DME spray cases, and comparison with experimental drop size data. Also the experimental data used did not present data for the evaporation of the droplets for which the spray model can take into account through source terms in equation (3); this will be explored.

Overall, the model is applicable to DME spray tip penetration studies.

Conclusions

A moments based spray model initially developed for simulating diesel spray cases has been applied to the prediction of DME spray tip penetration. The results, compared with existing experimental data, indicate that the model can be used for the evaluation of DME spray tip penetration. Generally, the model over predicts the fuel tip penetration at the start of injection and under predicts the spray tip penetration at the end of injection for the cases tested. Some work has started on evaluating the initial injection parameters in the model with respect DME sprays. Further work might be required with the drag and break up models, and cases of droplet evaporation need to be considered.

Acknowledgements

The author holds the University of Wolverhampton ERAS 2011/12 Fellowship, which partly supported this work.

Nomenclature

$n(r)$	Number Size Distribution
Q	Droplet Moment
Q_0	Total Number
Q_1	Sum of Radii, m
Q_2	Sum of Squares of Radii, m^2
Q_3	Sum of Cubes of Radii, m^3
r	Radius, m
t	Time, s
U	Velocity, ms^{-1}
x	Coordinate Direction, m

Greek Symbols

ν_l	Liquid viscosity, m^2s^{-1}
ε	Dissipation Rate, m^2s^{-3}
α	Nondimensional size parameter

Subscripts

32	Sauter mean
i	Moment index
i, j	Velocity component
l	Liquid

Acronyms

DME	Dimethyl Ether
DDM	Discrete Droplet Model
NO_x	Mono-nitrogen oxides NO and NO_2

References

[1] Ying, W., Langboa, Z., Zhongji, Y., and Hongyi, D., *Proceedings of the Institution of Mechanical Engineers, Part D: Journal of Automobile Engineering* 219(2): 263-269 (2005).

[2] Huang, Z.H., Wang, H.W., Chen, H.Y. Zhou, L.B., and Jiang, D.M., *Proceedings of the Institution of Mechanical Engineers, Part D: Journal of Automobile Engineering* 213(6): 647-652 (1999).

[3] Wang, H.W., Zhou, L.B., Jiang, D.M., and Huang, Z.H., *Proceedings of the Institution of Mechanical Engineers, Part D: Journal of Automobile Engineering* 214(1): 101-106 (2000).

[4] Lee, S-W., Murata, Y., and Daisho, Y., *Proceedings of the Institution of Mechanical Engineers, Part D: Journal of Automobile Engineering* 219(1): 97-102 (2005).

[5] Dukowicz, J.K., *Journal of Computational Physics* 35(2): 229-233 (1980).

[6] Kim, H.J., Duh, H.K., and Lee, C.S., *Proceedings of the Institution of Mechanical Engineers, Part D: Journal of Automobile Engineering* 223(10): 1351-1359 (2009).

[7] Park, S.H., Kim, H.J., and Lee, C.S., *Fuel* 89(10): 3001-3011 (2010).

[8] Wen, H., Liu, Y-C., Wei, M-R., and Zhang, Y-C., *Journal of Zhejiang University Science* 6A(4): 276-282 (2005).

[9] Emekwuru, N.G., and Watkins, A.P., *SAE Technical Paper 2011-01-1843, JSAE 20119080* (2011).

[10] Emekwuru, N.G., *SAE Technical Paper 2012-01-1260* (2012).

[11] Emekwuru, N.G., and Watkins, A.P., *Atomization and Sprays* 20(6): 467-484 (2010).

[12] Emekwuru, N.G., and Watkins, A.P., *Atomization and Sprays* 20(8): 653-672 (2010).

[13] Kim, S.C., Hwang, J.S., Ha, J.S., and No, S.Y., *Proceedings of the International Conference on Liquid Atomization and Spray Systems (ICLASS)*, Sorrento, Italy, July 13-17, 2003.

[14] Emekwuru, N.G., *Using the General Gamma Distribution to Represent the Droplet Size Distribution in a Spray Model*, Hydrodynamics-Theory and Model, Zheng, J-H (Ed.). InTech, 2012. Available from: http://www.intechopen.com/books/hydrodynamics-theory-and-model/using-the-general-gamma-distribution-to-represent-the droplet-size-distribution-in-a-spray-model

[15] Launder, B.E., and Spalding, D.B., *Mathematical Models of Turbulence*, Academic Press, London, 1972.

[16] Schihl, P., Bryzik, W., and Atreya, A., *SAE Technical Paper 960773* (1996).

[17] Sazhin, S.S., Feng, G., and Heikal, M.R., *Fuel* 80(15): 2171-2180 (2001).

[18] Hiroyasu, H., Kadota, T., and Arai, M., *Supplementary Comments: Fuel Spray Characterization in Diesel Engines, in: Combustion modelling in reciprocating engines*, Edited by Mattavi, J.N, and Amann, C.A.: 369-408. Plenum Press, 1980.

[19] Wakuri, Y., Fujii, M., Amitani, T., Tsuneya, R., *Bulletin of JSME* 3(9): 123-130 (1960).

[20] Dent, J.C., *SAE Technical Paper 710571* (1971).

[21] Melville, W.K., Bray, K.N.C., *International Journal of Heat and Mass Transfer* 22(5): 647-656 (1979).